Int J Clin Exp Pathol 2014;7(5):2019-2031
www.ijcep.com /ISSN:1936-2625/IJCEP0000227

Original Article

Role of far upstream element binding protein 1 in colonic epithelial disruption during dextran sulphate sodium-induced murine colitis

Qiyun Tang[1*], Weiwei Xia[2*], Qianqian Ji[2], Runzhou Ni[2], Jian'an Bai[1], Liren Li[2], Yongwei Qin[3]

[1]Department of Gastroenterology, The First Affiliated Hospital of Nanjing Medical University, 300 Guangzhou Road, Nanjing 210000, Jiangsu Province, People's Republic of China; [2]Department of Gastroenterology, Affiliated Hospital of Nantong University, 20 Xisi Road, Nantong 226001, Jiangsu Province, People's Republic of China; [3]Department of Pathogen Biology, Nantong University Medical College, 19 Qixiu Road, Nantong 226001, Jiangsu Province, People's Republic of China. [*]Equal contributors.

Received March 13, 2014; Accepted April 26, 2014; Epub April 15, 2014; Published May 1, 2014

Abstract: Aim: Intestinal epithelial barrier is essential for maintaining normal intestinal homeostasis; its breakdown leads to chronic inflammatory pathologies, such as inflammatory bowel diseases. Far upstream element binding protein 1 (FBP1) has been reported to play an important role in cell apoptosis and proliferation. We aimed to investigate the expression and the role of FBP1 in dextran sodium sulphate (DSS)-induced experimental colitis. Methods: Mice experimental colitis model was established by administration of DSS, and the expression and localization of FBP1 was examined using Western blot and immunohistochemistry. Colon epithelial cell line HT-29 was used to determine the role of FBP1. *In vitro* study, the expression of FBP1 was determined in HT-29 cells stimulated with tumor necrosis factor α (TNF-α). HT-29 cells were transfected with FBP1 siRNA and then measured for viability. Results: Significant decreasing of FBP1 expression was found in mice colitis. In addition, FBP1 was cleaved and translocated from nucleus to cytoplasm during apoptosis. Downregulated expression of FBP1 induced cell cycle arrest. Conclusions: We demonstrate that apoptosis-mediated cleavage of FBP1 and its decreased expression in epithelial cells induces cell cycle arrest, which may play an important role in colonic epithelial disruption.

Keywords: Colitis, intestinal epithelial cells, FBP1

Introduction

Inflammatory bowel disease (IBD), including both colitis and ileitis, is a chronic, relapsing, and remitting inflammatory dysfunction, which involving the mucosal layer of the colon and rectum [1]. It has been a worldwide health-care problem with a continually increasing incidence. The etiology of IBD is complex and incompletely understood. As researchers deepen their knowledge regarding the mechanisms underlying the pathogenesis of IBD, emerging evidence has revealed that the intestinal epithelium plays a central role [2]. Intestinal epithelial cells (IECs) which are the major compositions of intestinal epithelium are the primary cell type coming into contact with the external environment and act as the host's first line of the defense against potential harmful stimulants. IECs produce the mucus layer covering the entire length of the intestinal tract, whose role is to further protect the mucosal surface from harmful molecules and bacteria, and reinforce the overall intestinal barrier. Moreover, IECs also represent a core element of innate immunity within the gut mucosa, displaying a wide array of immune functions [3]. As such, IECs play an important role in maintaining the integrity of gut barrier and normal mucosal immune homeostasis. One form of epithelial cell injury in the inflamed colonic mucosa has been reported to involve the apoptosis of these cells [4]. Increased IEC apoptosis has been detected at the acute inflammatory sites in IBD [5, 6], which can disrupt intestinal mucosal integrity and barrier function and lead to other changes associated with colitis [7]. Since the apoptosis level of intestinal epithelial cells

increases during acute inflammation, the proliferation of epithelial cells is necessary to supply the reduction of intestinal cell library. The further decrease of the proliferation of intestinal epithelium, along with the increase of apoptosis, contributes to the injury of the epithelial barrier. However, molecular mechanisms that regulate intestinal epithelial barrier during IBD are incompletely understood.

Far upstream element binding protein (FBP) family includes three members which have been ascribed different functions in gene regulation [8, 9]. The human FBP1 gene, also known as FUBP1, encodes a 644-amino acid protein with three well-defined domains: an amphipathic helix N-terminal domain, a tyrosine-rich C-terminal transactivation domain and a DNA-binding central domain [10]. FBP1 was first identified as a DNA-binding protein that regulates c-Myc gene transcription [11]. In recent years, mounting evidence suggests that FBP1 acts as an RNA-binding protein and regulates mRNA translation or stability of genes [12]. During retroviral infection, FBP1 binds to and mediates replication of RNA from Enterovirus 71 [13]. In addition, FBP1 is also an important oncoprotein overexpressed in several human carcinomas, which promotes cell proliferation in a cell cycle-dependent pathway [14, 15]. Undoubtedly, FBP1 is a multifunctional protein. Previous studies reported that as a nuclear protein, FBP1 is cleaved by caspase-3 and -7 during apoptosis induced by various stimuli, which leads to FBP1 translocation from the nucleus to the cytoplasm [16]. Hypothetically, since that IEC apoptosis increases at the acute inflammatory sites in IBD might cause the change of FBP1 expression, the intestinal epithelial barrier would be destructed by the altered protein expression.

To clarify the mechanisms responsible for IBD development, a variety of experimental models for IBD has been developed, including a spontaneous colitis model, induced colitis models, as well as transgenic and knockout colitis models [17, 18]. Dextran sulfate sodium (DSS) has been used as one model to induce experimental colitis, which is often used to model the epithelial damage and a robust inflammatory response in IBDs. The aim of this study was to investigate the expression and role of FBP1 in colonic epithelial disruption during DSS-induced mice colitis.

Materials and methods

Animals and experimental colitis

Experiments were performed in accordance with National Institutes of Health Guidelines for the Care and Use of Laboratory Animals (National Research Council, 1996, USA) and were approved by the Chinese National Committee to Use of Experimental Animals for Medical Purposes, Jiangsu Branch. We obtained seven- to eight-week-old female C57Bl/6 mice (n = 22) weighing 18-20 g from the Experimental Animal Center of Nantong University. Both control group (n = 9) and experimental group (n = 13) of mice were maintained under specific pathogen-free conditions and given free access to food. Control mice were given normal drinking water, while 4% dextran sulfate sodium (4% (w/v) DSS; molecular weight, 36,000-50,000; MP Biomedicals) was contained in the water of experimental group from day 0 until day 7. And they were sacrificed on day 7 (n = 5). For recovery studies, DSS was administered for the first 7 days as indicated, then DSS was removed from the drinking water and mice (n = 5) were sacrificed 7 days after cessation of DSS treatment. Additional experimental mice (n = 3) were sacrificed on day 0. The control mice (n = 3 per time point) were respectively sacrificed on day 0, 7, 14.

Assessment of colitis activity

To examine the severity of colitis, we evaluated the body weight, disease activity index (DAI), and colon length. The DAI was determined by scoring changes in animal weight, occult blood, positivity, gross bleeding, and stool consistency. We used five grades of weight loss (0, no loss or weight gain; 1, 1-5% loss; 2, 5-10% loss; 3, 10-20% loss; 4, 20% loss), three grades of stool consistency (0, normal; 2, loose; and 4, diarrhea), and three grades of occult blood (0, negative; 2, occult blood-positive; and 4, gross bleeding). After determination of the DAI, mice were euthanized, the entire colon was removed from the cecum to the anus, and the colon length was measured as an indirect marker of inflammation.

Cell culture and stimulation

The human colon epithelial cell line HT-29 was purchased from Cell library, China Academy of Science. HT-29 cells were grown in 1640 (GibCo

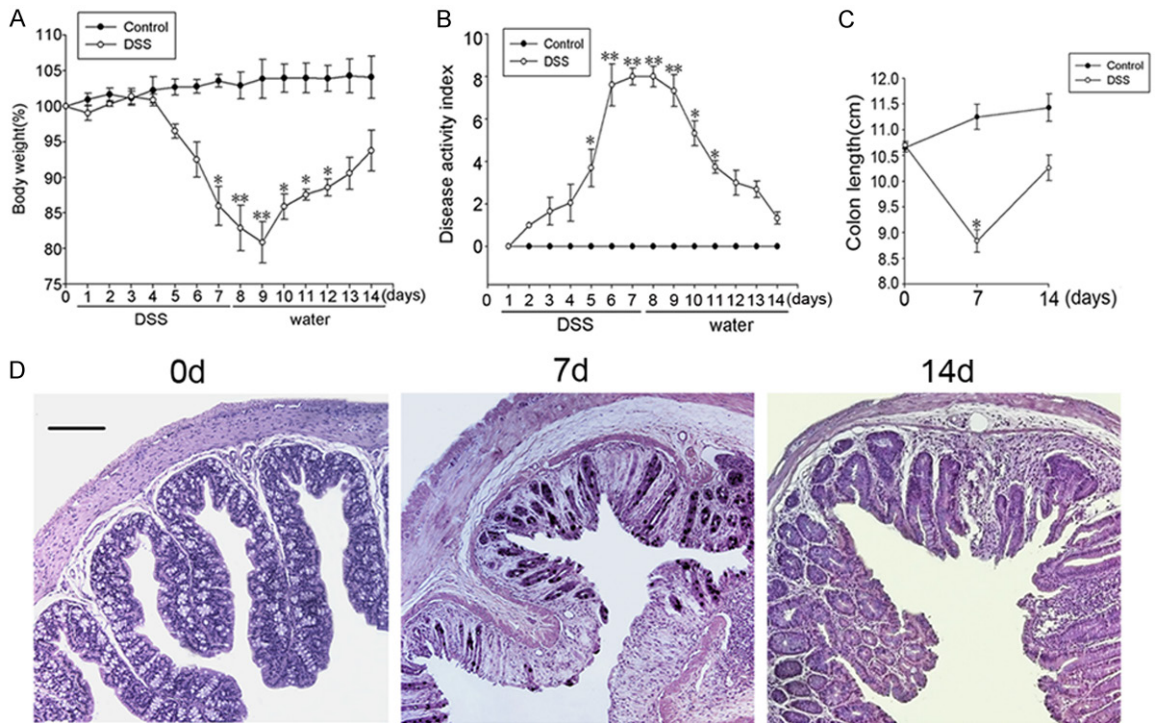

Figure 1. Multiple indicators is used to assess the success of DSS-induced colitis model. The changes of (A) body weight, (B) DAI, (C) colon length, and (D) colonic tissue structure by H&E-staining during the development of DSS-induced colitis in mice. Each value indicates the mean ± SE for 6 mouse. *(**)Significant difference at $P < 0.05$ ($P < 0.01$) compared with control mice receiving water alone. *Scale bar* column, 200 μm.

BRL, Grand Island, NY, USA) medium containing 10% fetal bovine serum (FBS), 100 U/ml penicillin, and 100 μg/ml streptomycin (GibCo BRL, Grand Island, NY, USA). Cultures were incubated at 37°C in a 95% air/5% CO_2 atmosphere. Cells were treated with different concentrations (1, 10, 100 ng/ml) of TNF-α (Sigma-Aldrich, USA). Cultured HT29 cells were collected, washed with phosphate buffer solution (PBS) and suspended in hypotonic buffer to achieve nuclear extracts. The cultured cells were homogenized, meanwhile nuclei were pelleted. Then we removed the cytoplasmic extracts and re-suspended nuclei in a low-salt buffer. A high-salt buffer was added to release soluble proteins from the nuclei, and the nuclei were removed by centrifugation. The nuclear extracts were dialyzed into a moderate salt solution.

Western blot analysis and antibodies

For Western blot analysis, colon tissues were dissected and flash-frozen at -80°C. To prepare the lysates, frozen samples were weighed and minced on ice. The samples were homogenized in lysis buffer (1% NP-40, 50 mmol/L Tris, Ph = 7.5, 5 mmol/L EDTA, 1% SDS, 1% sodium deoxycholate, 1% Triton-X100, 1 mmol/L PMSF, 10 μg/mL aprotinin, and 1 μg/mL leupeptin) and centrifuged at 12,000 rpm and 4°C for 20 min to collect the supernatant. Cell cultures for immunoblot were lysed with sodium lauryl sulfate loading buffer and stored at -80°C until use. After determining the protein concentration with the Bradford assay (Bio-Rad, Hercules, CA, USA), protein samples were subjected to SDS-polyacrylamide gel electrophoresis (SDS-PAGE) and transferred to a polyvinylidene difluoride filter (PVDF) membranes (Millipore, Bedford, MA, USA). The membranes were blocked with 5% fat-free milk in TBST (20 mM Tris, 150 mM NaCl, 0.05% Tween-20) for 2 h at room temperature, and then, the filters were washed with TBST for three times and incubated overnight with polyclonal antibody against using the primary antibodies against anti-FBP1 antibody (anti-mouse, 1:500; Santa Cruz), PCNA (anti-rabbit, 1:1000; Santa Cruz), Bcl-2 (anti-rabbit, 1:1000; Santa Cruz), cleaved-cas-

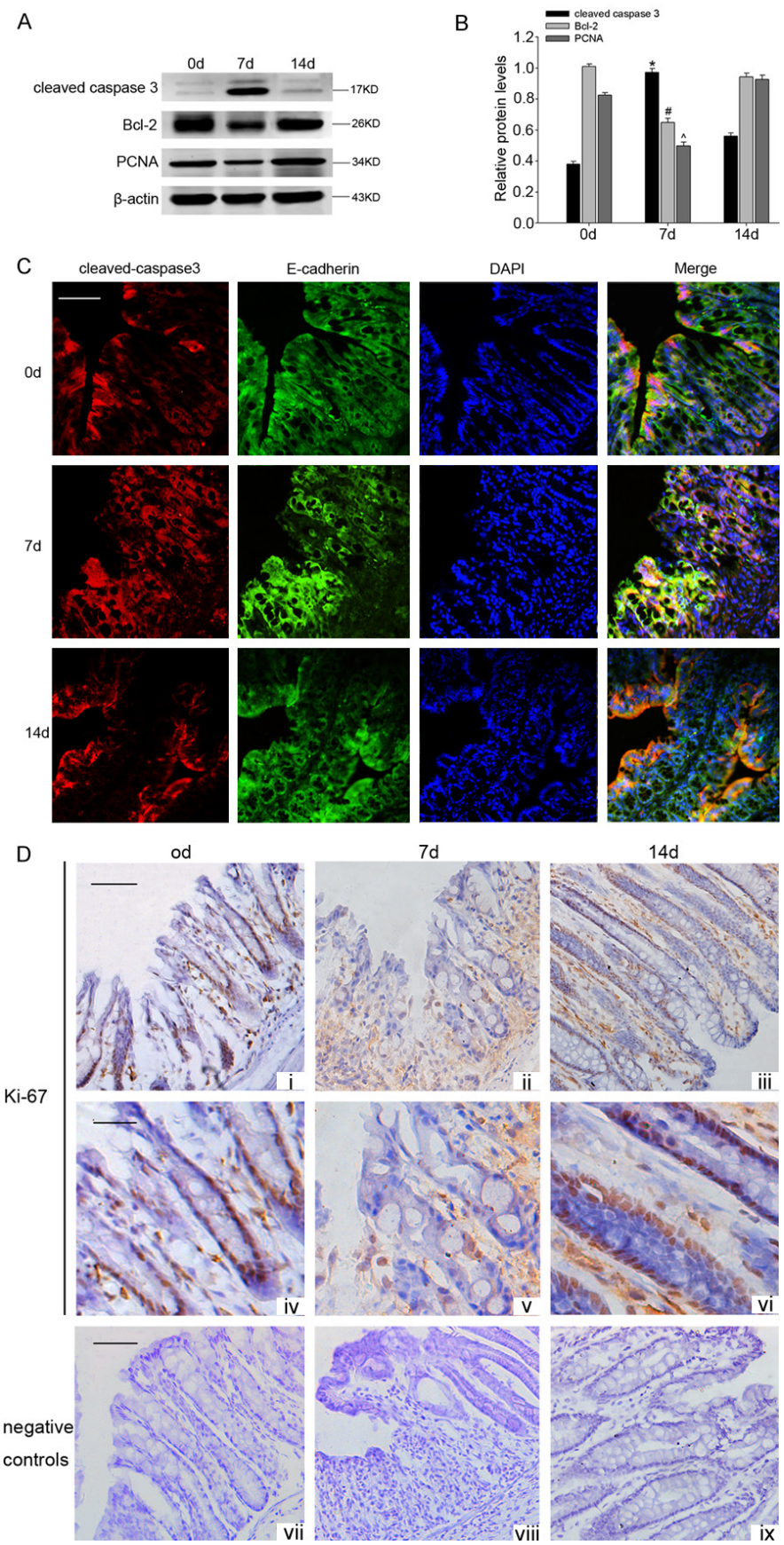

Figure 2. (A) Significant upregulation of cleaved-caspase 3, while downregulation of Bcl-2 and PCNA protein levels were detected in the mice fed DSS. β-actin served as the loading control. (B) The bar graph indicated the density of Bcl-2, cleaved-caspase 3 and PCNA versus β-actin at each time point. Data are presented as mean ± SEM. (n = 3, *, #, ^$P < 0.05$,). (C) Double immunofluorescent analysis showed that enhanced co-localizing of cleaved-caspase 3 with E-cadherin was observed after DSS administration. (D) Cell cycle analysis using an anti-Ki-67 antibody in the colonic crypts of DSS-induced colitis mice. There were some anti-Ki-67 positive cells in the lower part of the crypt before DSS administration (i, iv). However, the anti-Ki-67 positive cells were reduced in the mice fed DSS (ii, v). After stopped giving DSS, the anti-Ki-67 positive cells were increased significantly at day 14 (iii, vi). *Scale bar* (i-iii), 100 μm; *Scale bar* (iv-vi), 50 μm. (vii-ix: negative controls).

pase 3 (anti-rabbit, 1:500; Cell Signaling), cleaved PARP (anti-rabbit, 1:500; Cell Signaling), cyclin A (anti-rabbit, 1:1000; Santa Cruz), cyclin D1 (anti-rabbit, 1:1000; Santa Cruz), β-actin (anti-mouse, 1:500; Santa Cruz) at 4°C overnight. At last, the membrane was incubated with second antibody goat-anti-mouse or go-

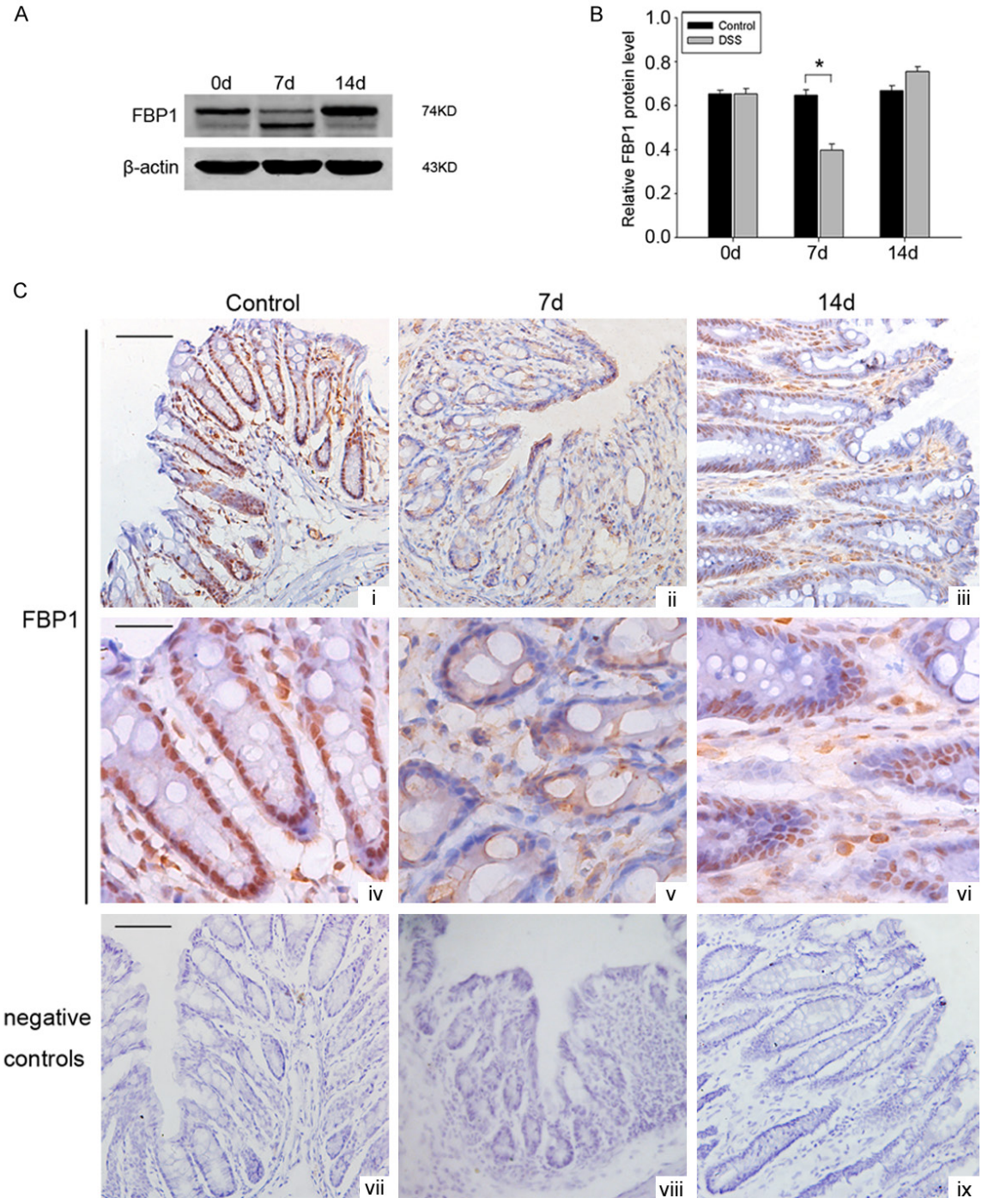

Figure 3. Changes of FBP1 expression in colonic tissues during mice experimental colitis. (A) Significant downregulation and cleavage of FBP1 was detected in the mice fed DSS in comparison to control mice. β-actin served as the loading control. (B) Quantitative analysis of the FBP1 protein level in mice colon with and without DSS treatment. The data are means ± SEM. (n = 3, *, $P < 0.05$; significantly different from the controlled group). (C) Immunohistochemistry with anti-FBP1 mouse monoclonal antibody on transverse cryosections of colonic tissues to identify the changes of FBP-1 immunoreactivity in DSS-induced mice colitis model at different time points. *Scale bar* (i-iii), 100 μm; *Scale bar* (iv-vi), 50 μm. (vii-ix: negative controls).

at-anti-rabbit conjugated horseradish peroxidase (1:2000, Southern-Biotech) for 2 h and visualized using an enhanced chemiluminescence system (ECL; Pierce Company, USA).

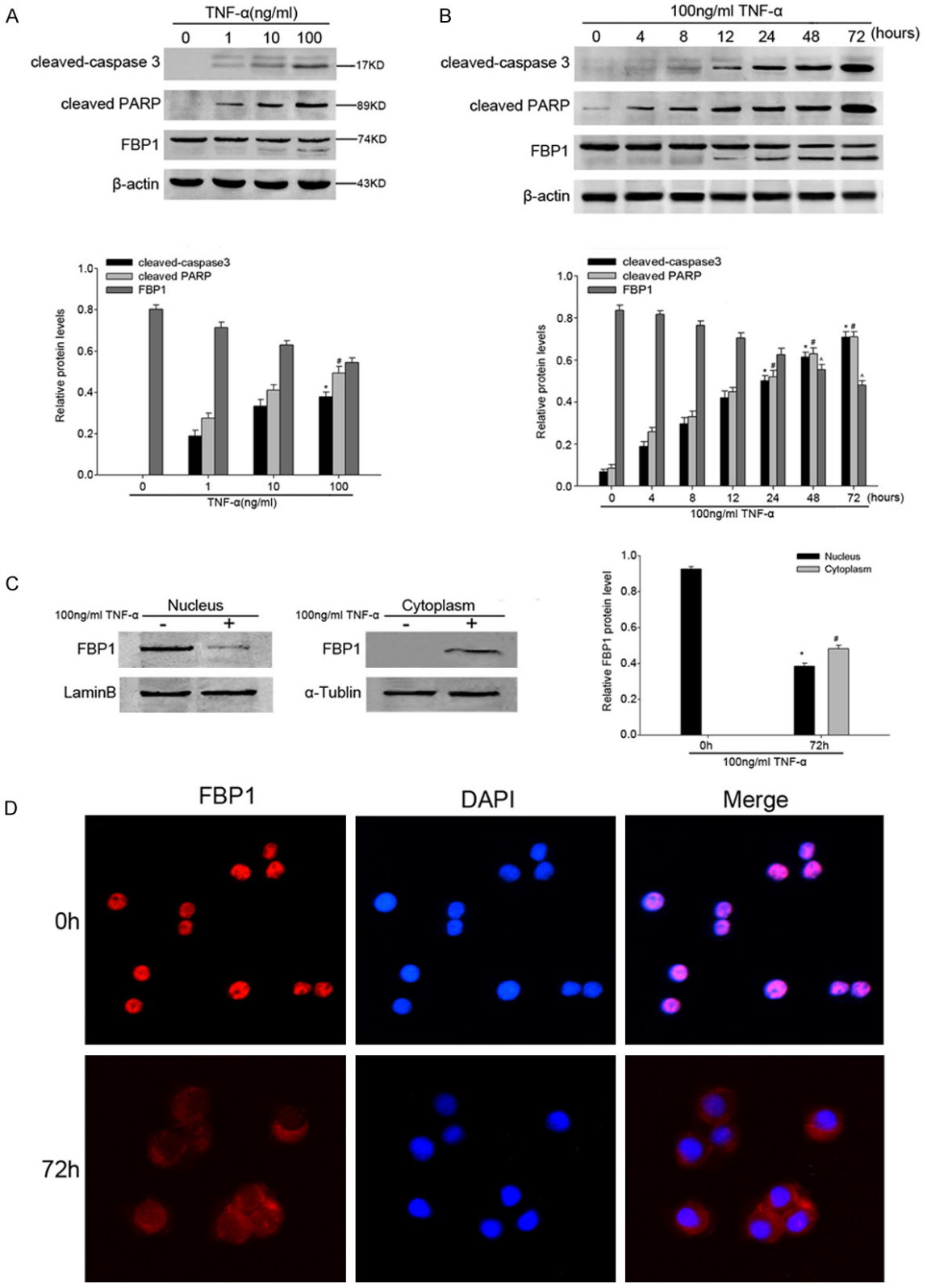

Figure 4. A. Cleaved-caspase 3, cleaved PARP and FBP1 protein in whole-cell lysates derived from different concentration of TNF-α treated (24 h) HT-29 cells shown by representative western blots of FBP1 and the loading control, β-actin. Data are presented as mean ± SEM of 3 independent measurements (*, #$P < 0.05$). B. A representative Western blot image showed that the expression of FBP1 in HT-29 cells that were subjected to 100 ng/ml TNF-α for

4, 8, 12, 24, 48, and 72 h. β-actin was used as a control for protein load and integrity. Data are presented as mean ± SEM of 3 independent measurements (*, #, ^$P < 0.05$). C. Nuclear and cytoplasmic FBP1 protein in TNF-α treated HT-29 cells shown by representative western blots. Lamin B and α-tublin were used as a loading control respectively. All the relative protein level was assessed by densitometric analysis (n = 3). Asterisks denote significant differences from the respective control ($*P < 0.05$). D. Immunofluorescence showed the change of subcellular localization of FBP1.

Immunofluorescent and immunohistochemical studies

Mice colon samples were freshly isolated and frozen in O.C.T (Sakura Finetek, USA) or fixed in 10% neutral buffered formalin and embedded in paraffin wax. Immunohistochemical studies were performed using paraffin-embedded sections (4 μm). All sections were deparaffinized, rehydrated, and thereafter, the sections were processed in 10 mM citrate buffer (pH 6.0) and heated to 121°C in an autoclave for 20 minutes to retrieve the antigen. After rinsing in PBS, sections were first treated with 3% hydrogen peroxide to block endogenous peroxidase activity, and then blocked by 1.5% normal goat serum for 20 min. For analysis for FBP1 and ki-67, sections were incubated 2 h at room temperature with primary antibody against FBP1 (diluted 1:800) and ki-67 (mouse; 1:1000; Santa Cruz Biotechnology, USA). All slides were processed using the peroxidase–anti-peroxidase method (DAKO, Hamburg, Germany). After rinsing in PBS, the peroxidase reaction was visualized by incubating the sections with the liquid mixture DAB (0.1% phosphate buffer solution, 0.02% diaminobenzidine tetrahydrochloride, and 3% H_2O_2). After rinsing in water, the sections were counterstained with hematoxylin, dehydrated, and cover slipped.

Additional sets of sections from mice were used for double immunofluorescence staining. Frozen sections were first blocked with 10% normal serum-blocking solution species the same as the secondary antibody, containing 3% (w/v) BSA and 0.1% Triton X-100 and 0.05% Tween-20 2 h at RT in order to avoid unspecific staining. Then, the sections were double stained with primary antibodies against cleaved-caspase 3 (anti-mouse, 1:200) and anti-E-cadherin (anti-rabbit, a marker of epithelial cells, 1:100, Santa Cruz). Briefly, sections were incubated with both primary antibodies overnight at 4°C, subsequently with secondary antibodies (donkey anti-rabbit Alexa Fluor® 488, 1:500; donkey anti-mouse Alexa Fluor® 568, 1:1,000) (both from Life Technologies Corporation, Paisley, UK) for 2 h at room temperature. To show the nucleus of cells, sections were counterstained with 4, 6-diamidino-2-phenylindole (DAPI; 0.1 mg/ml; Sigma Chemical Co., St. Louis, MO, USA) for 40 min at 30°C. The stained sections were examined under a Leica fluorescence microscope (Leica, DM 5000B; Leica CTR 5000; Germany).

To perform cell immunofluorescent staining, cells were fixed in formaldehyde for 1 h at room temperature. After washing with 1 × PBS, cells were permeabilized with 0.05% Triton X-100 in 1 × PBS for 15 min and incubated with preblock buffer (3% BSA, 0.02% Triton X-100 in 1 × PBS) for 15 min before being probed with primary antibodies [19]. And then cells were stained with anti-FBP1 antibody (anti-mouse, 1:200) at 4°C overnight, followed by secondary antibody (donkey anti-mouse Alexa Fluor® 568, 1:1000) for 2 h at room temperature. Nuclei were stained with DAPI (1:1000, Santa Cruz).

siRNA-mediated reduction of FBP1 expression

HT-29 cells were seeded in 6-well plates at a density of 400,000 cells per well in 1640 medium with glutamax supplemented with 1% fetal bovine serum. After 4 h, medium was replaced by serum-free medium. For transient transfection, the FBP1 siRNA vector or the non-specific vector was transfected using lipofectamine 2,000 and plus reagent in OptiMEM (Invitrogen). The target of FBP1 siRNA was 5'-AUACAGAUAGCUCCUGACA-3', while the control target was 5'-UUCUCCGAACGUGUCACGU-3'. Transfected cells were cultured for 48 h before using.

Cell cycle analyses

For cell cycle analysis, HT-29 cells were fixed in 70% ethanol overnight at 4°C and then incubated with 1 mg/ml RNase A for 20 min. Subsequently, cells were stained with propidium iodide (PI, 50 lg/ml) (Becton–Dickinson, San Jose, CA, USA) in PBS-Triton 9100 for an additional 20 min at 4°C and analyzed by a Becton-Dickinson flow cytometer BD FACScan (San Jose, CA, USA) and Cell Quest acquisition

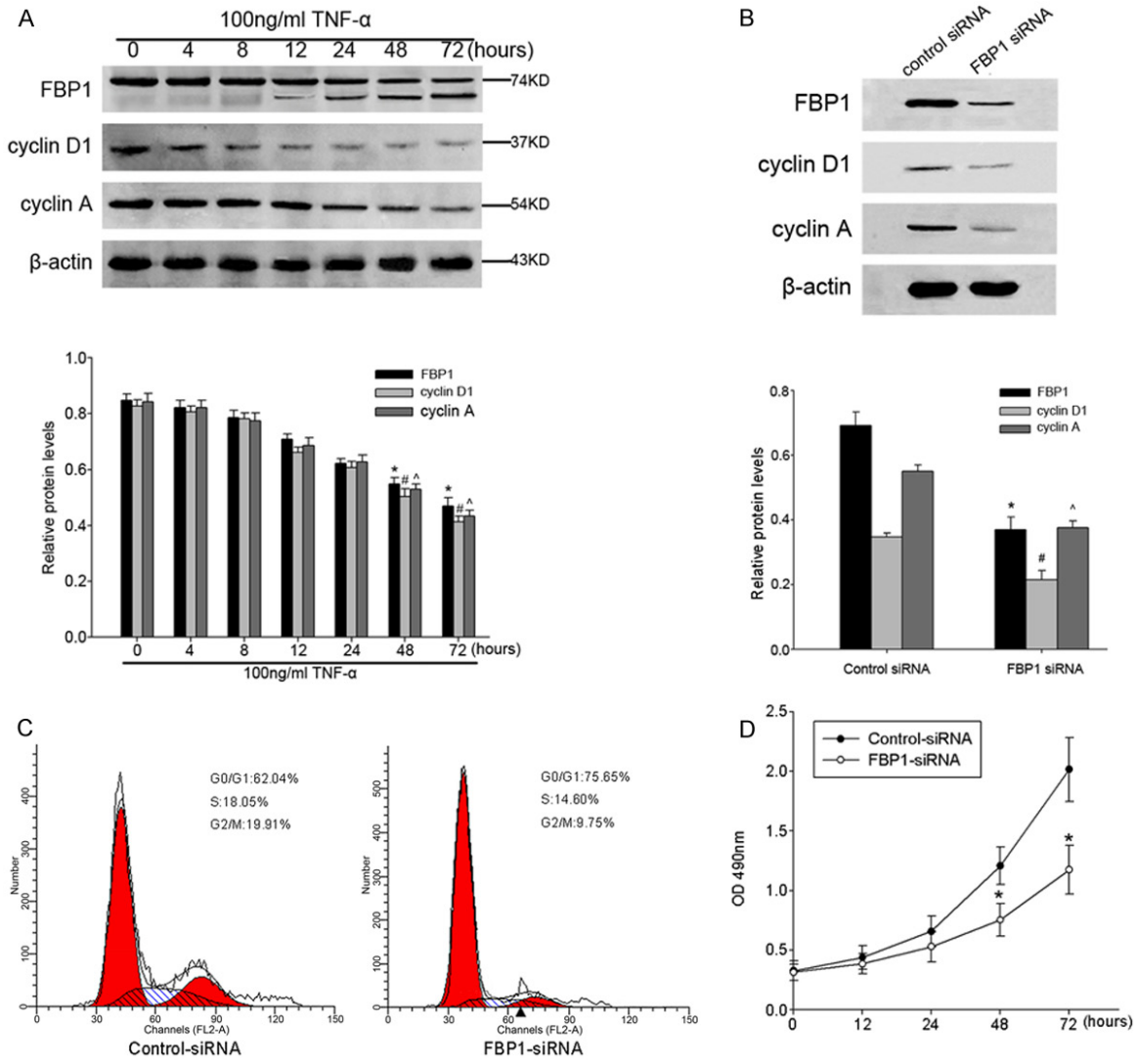

Figure 5. A. Upon TNF-α stimulation, FBP1/cyclin D1/cyclin A down-regulated concomitantly, reached the minimum at 72 h. The *bar chart* indicated the density of FBP1/cyclin D1/cyclin A versus β-actin. Data are presented as mean ± SEM of 3 independent measurements (*, #, ^$P < 0.05$). B. A representative Western blot image showed that FBP1, cyclin A, and cyclin D1 protein expression in the cells were decreased by treatment of FBP1 siRNA and control siRNA. A *bar chart* demonstrated the relative protein expression of FBP1, cyclin A, and cyclin D1 in HT-29 cells by control siRNA or FBP1 siRNA as measured by Western blot analysis. Data are presented as mean ± SEM of 3 independent measurements. β-actin was used as internal control for Western blot analysis (*, #, ^$P < 0.05$). C. Cell cycle analysis revealed an accumulation of cells in the G0/G1 phase, a decreased population at the S phase from 18.05 to 14.60% and G2/M phase from 19.91 to 9.75% after transfection of FBP1 siRNA into the HT-29 cell line. D. The comparison in growth curves between the cells treated with FBP1 siRNA and control siRNA, as measured by CCK-8 assay. The experiments were repeated at least three times (*$P < 0.05$).

and analysis programs. Gating was set to exclude cell debris, cell doublets, and cell clumps. The results were gained from three independent experiments.

Cell Counting Kit (CCK) -8 assay

Cell proliferation was measured using the commercial CCK-8 kit in accordance with the manufacturer's protocol. Briefly, cells were seeded onto 96-well cell culture cluster plates (Corning, Corning, NY, USA) at a concentration of 5×10^4 cells/well in volumes of 100 μl and grew overnight. CCK-8 reagents (Dojindo, Kumamoto, Japan) were added to a subset of wells under different treatments. Cells were incubated for another 1 h at 37°C, and absorbance was

quantified using an automated plate reader. Absorbency was measured at a test wavelength of 490 nm and a reference wavelength of 630 nm using a microplate reader (Bio-Rad). The experiments were repeated at least three times.

Statistical analysis

All values were expressed as mean ± SEM. Data were compared by using the Student's t test. $P < 0.05$ was required for statistical significance. Each experiment consisted of at least three replicates per condition. SEM refers to the standard error of the mean.

Results

Mouse DSS-induced colitis

We investigated the susceptibility of mice to DSS-induced colitis by analyzing the change of body weight, DAI, and the histology of the colon. The body weight of mice began to decline at day 3 and reached to the minimum at day 8. Afterwards, as stopped giving DSS, mice body weight gradually increased (**Figure 1A**). The clinical scores for weight loss, bleeding and diarrhea were added to produce the DAI. After giving DSS, the DAI of mice was gradually increased. Similarly, after stopping administration, DAI gradually decreased (**Figure 1B**). As shown in **Figure 1C**, colon length was significantly reduced after 7 days of DSS administration and was shorter than control mice at day 14. H&E-stained colon sections showed that DSS-induced inflammatory cell infiltration within the lamina propria, focal loss of crypts, depletion of epithelial cells, disseminated fibrosis. At day 14, the intestinal crypts proliferated obviously and intestinal mucosal layer basically repaired (**Figure 1D**).

Increased apoptosis and decreased proliferation of colonic epithelium in DSS-induced colitis

As DSS is toxic to mucosal epithelial cells and can affect the epithelium by inhibiting proliferation and inducing apoptosis in mice [20], and eventual dysfunction of mucosal barrier leads to mucosal inflammation, we examined the apoptosis and proliferation of colonic epithelium in DSS-induced colitis. Western blot was performed to examine the expression of cleaved-caspase 3, Bcl-2 and PCNA. As shown in **Figure 2A**, the expression of cleaved-caspase 3 increased markedly after DSS administration, while the expression of anti-apoptosis protein Bcl-2 was lower than normal. In addition, the marker of proliferation, PCNA, was lowly expressed in mice with colitis compared with normal mice. We then explored the apoptosis and proliferation of colonic epithelium by immunofluorescent and immunohistochemical analyses. Immunofluorescent analysis showed that enhanced co-localizing of cleaved-caspase 3 with E-cadherin, a marker of epithelial cells, was observed after DSS administration (**Figure 2C**). We observed the cell cycle status of the epithelium using immunostaining with an anti-mouse Ki-67 antibody, which indicates the activated phases of the cell cycle (G1, S, G2, and M phases). There were some anti-Ki-67 positive cells in the lower part of the crypt before DSS administration (**Figure 2Di**, **2Div**). However, the anti-Ki-67 positive cells were reduced in the mice fed DSS (**Figure 2Dii**, **2Dv**). While after stopped giving DSS, the anti-Ki-67 positive cells were increased significantly at day 14 (**Figure 2Diii**, **2Dvi**). These results suggested that after DSS administration, the apoptosis of the epithelial cells increases and cell cycle arrests. However, the precise mechanisms remain unknown.

Expression and localization of FBP1 in colonic epithelium

Previous researches have shown that FBP1 is cleaved by executor caspases during apoptosis. The caspase-mediated cleavage of FBP1 leads to its decreased presence in the nucleus [16]. In addition, it had been reported that loss of FBP1 arrested cellular proliferation [21]. Thus, we hypothesized that FBP1 might be relevant to colonic epithelial disruption during DSS-induced murine experimental colitis. We investigated the temporal expression patterns of FBP1 in mice colonic mucosa from DSS-induced colitis model, western blot analysis and immunohistochemistry were employed. The results of western blot analysis indicated that the level of FBP1 protein was markedly decreased in DSS-induced colitis model. In addition, the results showed an obvious cleaved FBP1. While after stopped giving DSS, the expression of FBP1 increased again at day 14 (**Figure 3A**, **3B**). To identify the changes of FBP1 immunoreactivity in DSS-induced mice colitis model, we then performed immunohistochemistry with anti-FBP1 mouse monoclonal anti-

body on transverse cryosections of colonic tissue. The nucleus of intestinal epithelium of controls showed a strong positive staining for FBP1. While 7 days after DSS administration, the immunostaining of FBP1 in the nucleus was practically undetectable, it mainly located in cytoplasm of epithelium. At day 14, the immunostaining of FBP1 located in the nucleus of epithelium again (**Figure 3C**). Taken together, these results demonstrated clearly that the expression of FBP1 in the nucleus of epithelial cells decreased in DSS-induced mice colitis.

TNF-α-mediated epithelial cell apoptosis induced cleavage of FBP1 and affected cellular localization of FBP1

Results of mice *in vivo* studies have demonstrated that apoptosis of colonic epithelium increased in DSS-induced mice colitis, while the expression of FBP1 decreased and FBP1 translocated to cytoplasm during active inflammation. Thus, we hypothesized that the translocation of FBP1 was induced by epithelium apoptosis. To confirm this postulation, we performed *in vitro* experiments using the human IEC line HT-29 cells incubated with tumor necrosis factor α (TNF-α), a key cytokine which was involved in the pathogenesis of IBD and could stimulate cell apoptotic pathways in IECs [22]. First of all, we incubated HT-29 cells with different concentration (1, 10, 100 ng/ml) of TNF-α for 24 h to determine the most appropriate stimulant concentration to induce apoptosis. When using 100 ng/ml TNF-α, the abundance of cleaved-caspase 3 and the well-known caspase substrate, cleaved PARP reached the peak, consistently, it showed a remarkable cleavage and decrease of FBP1 expression (**Figure 4A**). Based on this observation, we continued with a concentration of 100 ng/ml TNF-α in all of our subsequent experiments. We treated HT-29 cells for 4, 8, 12, 24, 48 and 72 h, and TNF-α decreased FBP1 protein expression levels significantly after 24 h and 72 h incubations, at the same time, Western blot showed the up-regulation of cleaved-caspase 3 and cleaved PARP in a time-dependent manner. In addition, the cleavage of FBP1 occurred along with the expression of cleaved-caspase 3 (**Figure 4B**). We then examined whether FBP1 is translocated during apoptosis. We collected separate cytoplasmic and nuclear protein lysates from HT-29 cells after TNF-α treatment for 72 h. The results showed that in controls, FBP1 protein expressed in nucleus, while after 72 h of TNF-α stimulation, FBP1 protein levels decreased significantly in nuclear compartment, but elevated in the cytoplasmic compartment (**Figure 4C**). Furthermore, immunofluorescence exhibited the translocation of FBP1 from nucleus to cytoplasm after apoptotic stimuli (**Figure 4D**). All these results demonstrated that FBP1 was cleaved during apoptosis by TNF-α stimuli, and cleavage of FBP1 resulted in a decrease in its overall nuclear level.

Depletion of FBP1 arrested cell cycle of IECs

Several studies have reported that FBP1 regulated the expression of some cell cycle inhibitors, which demonstrated that loss of FBP1 promoted the expression of several cell cycle inhibitors [14]. Thus, we hypothesized that down-regulation of FBP1 might also affect cell cycle of IECs in DSS-induced colitis. TNF-α induced epithelial cell apoptosis, which caused cleavage of FBP1 and a decrease in its overall nuclear level. *In vitro* experiments, we found that the expression of cell cycle markers such as cyclin A and cyclin D1 down-regulated in a time-dependent manner after TNF-α stimulus, which was similar with FBP1 expression (**Figure 5A**). To further explore whether the down-regulation of these cell cycle marker was relevant to the FBP1 expression, HT-29 cells were transiently transfected with FBP1 siRNA or control siRNA constructs. Forty-eight hours after transfection, the efficiency of FBP1 siRNA-mediated down-regulation was assessed by Western blot analysis. It was found that the expression of FBP1 was significantly reduced in FBP1 siRNA cells compared with control siRNA group (**Figure 5B**). The expression of cyclin D1 and cyclin A were correlated positively with FBP1 expression. At the same time, to determine whether the cell cycle distribution was changed after knockdown of FBP1 in HT-29 cells, we performed flow cytometry 48 h after the FBP1 siRNA transient transfection. Cell cycle analysis revealed an accumulation of cells in the G0/G1 phase, a decreased population at the S phase from 18.05 to 14.60% and G2/M phase from 19.91 to 9.75% after transfection of FBP1 siRNA into the HT-29 cell line (**Figure 5C**), suggesting that loss of FBP1 could induce cell cycle arrest. In addition, we assessed the effects of FBP1 knocked down on HT-29 cell proliferation by CCK-8 assays. The result showed that HT-29 cells treated with siRNA

exhibited a significant deceleration of cell proliferation rate compared with the control siRNA (**Figure 5D**). Taken together, these results demonstrated that siRNA targeting FBP1 exhibited inhibition of S-phase and M-phase entry, as well as a specific inhibitory effect on HT-29 cell line growth.

Discussion

In our study, 4% DSS induced severe colitis for a short period. The oral administration of DSS induced several symptoms including diarrhea and weight loss, and histological changes of the colonic mucosa including inflammation and crypt loss. We detected that DSS administration certainly induced apoptosis but significantly reduced the anti-Ki-67 positive cell ratio as compared to the control mice. These results were accordance with previous studies [23, 24]. The increased apoptosis and cell cycle arrest might lead to a breakdown of the epithelial barrier function at a very early phase of colitis, which might lead to the mucosal invasion of intestinal bacterial and their toxins. However, the precise mechanisms responsible for this apoptosis and cell cycle arrest remain unknown. In this study, we presented new insight into the molecular mechanisms for epithelial barrier disruption by FBP1 in DSS-induced experimental colitis.

In DSS-induced experimental colitis, we detected that FBP1 was cleaved and translocated from nucleus to cytoplasm in the colonic mucosa epithelium. As a transcription regulator, FBP1 is primarily located in the nucleus where it exerts multiple biological function. The nuclear localization of FBP1 protein is driven by three nuclear localization signals (NLSs), one in each of its N-terminal, central and C-terminal domains. Previous study reported that FBP1 localized in cytoplasm in apoptotic cells [16]. Such localization is related to the fact that FBP1 is a substrate of caspase-3 and -7, which cleave FBP1 at the DQPD consensus site located in the N-terminal NLS. When cells suffered from apoptotic stimuli, the caspase-mediated cleavage of FBP1 led to its decreased presence in the nucleus, accompanied by the marked downregulation of its various target gene. According to the above findings, we hypothesized that the cleavage of FBP1 in mice colitis may be due to the apoptosis of intestinal epithelial cells. To test this conjecture, we constructed a model of apoptosis in vitro with TNF-α stimulation. Previous study has confirmed that TNF is an important inducer of IEC apoptosis [25]. Our *in vitro* results demonstrated clearly that TNF-α-mediated epithelial cell apoptosis induced FBP1 cleavage and which contributed to its decreasing presence in the nucleus and translocating to the cytoplasm.

Since the apoptosis level of intestinal epithelial cells increased, the proliferative epithelial cells is necessary to supply the reduction of intestinal cell library after injury. However, we detected that proliferative epithelial cells were reduced in the mice fed DSS. The specific mechanism about this is not yet very clear. Several studies have reported that loss of FBP1 could arrest cell cycle. FBP1 was first identified as a DNA-binding protein that regulates c-Myc gene transcription through binding to the far upstream element in the promoter region 1.5 kb upstream of the transcription start site [26]. c-Myc is a master switch of cellular proliferation and this topic has been reviewed extensively elsewhere [27, 28]. Previous study has been reported that loss of FBP1 extinguished c-Myc expression [21, 29]. Decreased expression of c-Myc mRNA has been associated with prevention of G1-S phase transition and inhibition of cell proliferation [30, 31]. In addition, several studies reported that FBP1 regulated cell proliferation through c-Myc-independent mechanisms. For example, FBP1 downregulated p21 mRNA probably through AREs at the 3'-UTR [32]. p21 mRNA expression was significantly increased following stable FBP1 knockdown [14]. The p21 gene encodes an inhibitor of cyclin-dependent kinases and inhibits cell proliferation in general [33]. Moreover, ectopic expression of FBP1 may also induce the cell cycle inhibitor $p27^{Kip}$ by promoting its translation via IRES in the 5'-UTR [12]. All of these results demonstrated that downregulated expression of FBP1 in the nucleus and ectopic expression of FBP1 both promoted cell cycle arrest. In our study, we found that TNF-α-mediated HT-29 cell apoptosis induced cleavage of FBP1 which lead to downregulated expression of FBP1 in the nucleus and ectopic expression of FBP1. Moreover, knockdown of FBP1 in HT-29 cell line lead to cell cycle arrest and reduced cell growth. However, the mechanism that FBP1 regulates the cell cycle of IECs remains to be further studied.

In summary, our study demonstrated for the first time that intestinal epithelial cells apoptosis induced cleavage of FBP1, which could lead to cell cycle arrest and thus result in a breakdown of epithelial barrier function at a very early phase of colitis. Previous studies reported that repeated cycles of the oral administration of DSS in rats was able to induce an abnormal increase in the proliferation of colonic epithelial cells [34]. It is reasonable that the repair and/or proliferation processes might catch up with the progression of the DSS-induced apoptosis and cell cycle arrest. If animals were given repeated cycles of DSS administration, the colonic epithelium might undergo chronic inflammation, including subsequently increased proliferation. It is possible that this chronic colitis may lead to an increased incidence of colon cancer. In this study, we just investigated the expression and biological function of FBP1 at the early phase of mice colitis, whereas what functions FBP1 exerts in the pathogenesis of mice chronic colitis and IBD remains to be further studied.

Acknowledgements

This work was supported by Natural Science Foundation of China (81201252); Jiangsu Province's Key Provincial Talents Program (grant RC2011079); The project of the six talent summit of Jiangsu Province (grant 2009-B1-002).

Disclosure of conflict of interest

None.

Address correspondence to: Dr. Liren Li, Department of Gastroenterology, Affiliated Hospital of Nantong University, 20 Xisi Road, Nantong 226001, Jiangsu Province, People's Republic of China. Tel: +86-513-85051857; Fax: +86-513-85051896; E-mail: Larry-017@163.com; Dr. Yongwei Qin, Department of Pathogen Biology, Nantong University Medical College, 19 Qixiu Road, Nantong 226001, Jiangsu Province, People's Republic of China. Tel: +86-513-85051736; Fax: +86-513-85052307; E-mail: qinyongwei012-@163.com

References

[1] Gross KJ and Pothoulakis C. Role of neuropeptides in inflammatory bowel disease. Inflamm Bowel Dis 2007; 13: 918-932.

[2] Pastorelli L, De Salvo C, Mercado JR, Vecchi M and Pizarro TT. Central Role of the Gut Epithelial Barrier in the Pathogenesis of Chronic Intestinal Inflammation: Lessons Learned from Animal Models and Human Genetics. Front Immunol 2013; 4: 280.

[3] Maldonado-Contreras AL and McCormick BA. Intestinal epithelial cells and their role in innate mucosal immunity. Cell Tissue Res 2011; 343: 5-12.

[4] Iimura M, Nakamura T, Shinozaki S, Iizuka B, Inoue Y, Suzuki S and Hayashi N. Bax is downregulated in inflamed colonic mucosa of ulcerative colitis. Gut 2000; 47: 228-235.

[5] Hagiwara C, Tanaka M and Kudo H. Increase in colorectal epithelial apoptotic cells in patients with ulcerative colitis ultimately requiring surgery. J Gastroenterol Hepatol 2002; 17: 758-764.

[6] Di Sabatino A, Ciccocioppo R, Luinetti O, Ricevuti L, Morera R, Cifone MG, Solcia E and Corazza GR. Increased enterocyte apoptosis in inflamed areas of Crohn's disease. Dis Colon Rectum 2003; 46: 1498-1507.

[7] Schulzke JD, Bojarski C, Zeissig S, Heller F, Gitter AH and Fromm M. Disrupted barrier function through epithelial cell apoptosis. Ann N Y Acad Sci 2006; 1072: 288-299.

[8] Briata P, Forcales SV, Ponassi M, Corte G, Chen CY, Karin M, Puri PL and Gherzi R. p38-dependent phosphorylation of the mRNA decay-promoting factor KSRP controls the stability of select myogenic transcripts. Mol Cell 2005; 20: 891-903.

[9] Dean JL, Sully G, Clark AR and Saklatvala J. The involvement of AU-rich element-binding proteins in p38 mitogen-activated protein kinase pathway-mediated mRNA stabilisation. Cell Signal 2004; 16: 1113-1121.

[10] Duncan R, Collins I, Tomonaga T, Zhang T and Levens D. A unique transactivation sequence motif is found in the carboxyl-terminal domain of the single-strand-binding protein FBP. Mol Cell Biol 1996; 16: 2274-2282.

[11] Avigan MI, Strober B and Levens D. A far upstream element stimulates c-myc expression in undifferentiated leukemia cells. J Biol Chem 1990; 265: 18538-18545.

[12] Zheng Y and Miskimins WK. Far upstream element binding protein 1 activates translation of p27Kip1 mRNA through its internal ribosomal entry site. Int J Biochem Cell Biol 2011; 43: 1641-1648.

[13] Huang PN, Lin JY, Locker N, Kung YA, Hung CT, Huang HI, Li ML and Shih SR. Far upstream element binding protein 1 binds the internal ribosomal entry site of enterovirus 71 and enhances viral translation and viral growth. Nucleic Acids Res 2011; 39: 9633-9648.

[14] Rabenhorst U, Beinoraviciute-Kellner R, Brezniceanu ML, Joos S, Devens F, Lichter P, Rieker RJ, Trojan J, Chung HJ, Levens DL and Zornig M. Overexpression of the far upstream element binding protein 1 in hepatocellular carcinoma is required for tumor growth. Hepatology 2009; 50: 1121-1129.
[15] Ding Z, Liu X, Liu Y, Zhang J, Huang X, Yang X, Yao L, Cui G and Wang D. Expression of far upstream element (FUSE) binding protein 1 in human glioma is correlated with c-Myc and cell proliferation. Mol Carcinog 2013; [Epub ahead of print.
[16] Jang M, Park BC, Kang S, Chi SW, Cho S, Chung SJ, Lee SC, Bae KH and Park SG. Far upstream element-binding protein-1, a novel caspase substrate, acts as a cross-talker between apoptosis and the c-myc oncogene. Oncogene 2009; 28: 1529-1536.
[17] Mayer L. The development of animal models of inflammatory bowel disease. Int Rev Immunol 2000; 19: 77-90.
[18] Mizoguchi A. Animal models of inflammatory bowel disease. Prog Mol Biol Transl Sci 2012; 105: 263-320.
[19] Liu Y, Chen Y, Lu X, Wang Y, Duan Y, Cheng C and Shen A. SCYL1BP1 modulates neurite outgrowth and regeneration by regulating the Mdm2/p53 pathway. Mol Biol Cell 2012; 23: 4506-4514.
[20] Kim YH, Kwon HS, Kim DH, Shin EK, Kang YH, Park JH, Shin HK and Kim JK. 3,3'-diindolylmethane attenuates colonic inflammation and tumorigenesis in mice. Inflamm Bowel Dis 2009; 15: 1164-1173.
[21] He L, Liu J, Collins I, Sanford S, O'Connell B, Benham CJ and Levens D. Loss of FBP function arrests cellular proliferation and extinguishes c-myc expression. EMBO J 2000; 19: 1034-1044.
[22] Wang J and Fu YX. Tumor necrosis factor family members and inflammatory bowel disease. Immunol Rev 2005; 204: 144-155.
[23] Araki Y, Mukaisyo K, Sugihara H, Fujiyama Y and Hattori T. Increased apoptosis and decreased proliferation of colonic epithelium in dextran sulfate sodium-induced colitis in mice. Oncol Rep 2010; 24: 869-874.
[24] Tessner TG, Cohn SM, Schloemann S and Stenson WF. Prostaglandins prevent decreased epithelial cell proliferation associated with dextran sodium sulfate injury in mice. Gastroenterology 1998; 115: 874-882.
[25] Goretsky T, Dirisina R, Sinh P, Mittal N, Managlia E, Williams DB, Posca D, Ryu H, Katzman RB and Barrett TA. p53 mediates TNF-induced epithelial cell apoptosis in IBD. Am J Pathol 2012; 181: 1306-1315.
[26] Wierstra I and Alves J. The c-myc promoter: still MysterY and challenge. Adv Cancer Res 2008; 99: 113-333.
[27] de Nigris F, Sica V, Herrmann J, Condorelli G, Chade AR, Tajana G, Lerman A, Lerman LO and Napoli C. c-Myc oncoprotein: cell cycle-related events and new therapeutic challenges in cancer and cardiovascular diseases. Cell Cycle 2003; 2: 325-328.
[28] Morrish F, Isern N, Sadilek M, Jeffrey M and Hockenbery DM. c-Myc activates multiple metabolic networks to generate substrates for cell-cycle entry. Oncogene 2009; 28: 2485-2491.
[29] Chung HJ and Levens D. c-myc expression: keep the noise down! Mol Cells 2005; 20: 157-166.
[30] Heikkila R, Schwab G, Wickstrom E, Loke SL, Pluznik DH, Watt R and Neckers LM. A c-myc antisense oligodeoxynucleotide inhibits entry into S phase but not progress from G0 to G1. Nature 1987; 328: 445-449.
[31] Holt JT, Redner RL and Nienhuis AW. An oligomer complementary to c-myc mRNA inhibits proliferation of HL-60 promyelocytic cells and induces differentiation. Mol Cell Biol 1988; 8: 963-973.
[32] Xiao J, Zhang Z, Chen GG, Zhang M, Ding Y, Fu J, Li M and Yun JP. Nucleophosmin/B23 interacts with p21WAF1/CIP1 and contributes to its stability. Cell Cycle 2009; 8: 889-895.
[33] Abbas T and Dutta A. p21 in cancer: intricate networks and multiple activities. Nat Rev Cancer 2009; 9: 400-414.
[34] Inoue T, Murano M, Kuramoto T, Ishida K, Kawakami K, Abe Y, Morita E, Murano N, Toshina K, Nishikawa T, Maemura K, Shimamoto C, Hirata I, Katsu K and Higuchi K. Increased proliferation of middle to distal colonic cells during colorectal carcinogenesis in experimental murine ulcerative colitis. Oncol Rep 2007; 18: 1457-1462.